Available online at www.sciencedirect.com
SCIENCE DIRECT®
Biochemical and Biophysical Research Communications 322 (2004) 93–99
BBRC
www.elsevier.com/locate/ybbrc

Oligomerization of the SARS-CoV S glycoprotein: dimerization of the N-terminus and trimerization of the ectodomain

Xiaodong Xiao, Yang Feng, Samitabh Chakraborti, Dimiter S. Dimitrov *

Protein Interactions Group, LECB, CCR, NCI-Frederick, NIH, Frederick, MD 21702-1201, USA

Received 25 June 2004
Available online 3 August 2004

Abstract

Viral envelope glycoproteins are oligomeric and the quaternary structure is critical for their membrane fusion activity. Typically the transmembrane glycoproteins of class I fusion proteins contain the oligomerization domains and the surface glycoproteins (SU) are monomeric. However, it has been previously demonstrated [J. Biol. Chem. 277 (2002) 19727] that the SU of a murine hepatitis coronavirus (MHV) forms dimers, the dimerization domain overlaps the receptor-binding domain (RBD) and that this dimeric state is important for binding to receptor molecules that initiates entry into cells. We have previously expressed various soluble fragments of the SARS-CoV SU and identified stably folded fragments (residues 272–537) that contain the RBD [Biochem. Biophys. Res. Commun. 312 (2003) 1159]. Here, we further characterize these and other fragments in an attempt to identify possible dimerization domains and their role for membrane fusion. We demonstrate that the SU and a shorter 260-amino acid N-terminal fragment (residues 17–276), which folds independently, form dimers. In contrast to the previously characterized MHV SU dimerization, this fragment is upstream and distinct from the RBD. Its deletion abolished S-mediated cell membrane fusion but retained the SU-receptor-binding function indicating the possibility for a role in post-receptor binding steps of the virus entry mechanism. Interestingly, the whole soluble S ectodomain (Se) that contains the dimerization domain but not the transmembrane domain and the cytoplasmic tail forms trimers suggesting the existence of a trimerization domain in the TM subunit in its prefusion state that may lead to a conformation unfavorable for formation of higher-order multimeric structures. These results demonstrate the existence of SU dimers and Se trimers, and indicate the possibility for an unknown mechanism of their role in entry. They also further characterize the S-mediated membrane fusion and could be important for understanding the mechanisms of virus entry, and in the development of therapeutics and vaccines.

Keywords: SARS-CoV; S glycoprotein; S protein; S oligomerization; Membrane fusion

Viral envelope glycoproteins initiate entry of viruses into cells by binding to cell surface receptors followed by conformational changes leading to membrane fusion and delivery of the genome in the cytoplasm [1]. The spike (S) glycoproteins of coronaviruses are no exception and mediate binding to host cells followed by membrane fusion; they are major targets for neutralizing antibodies and form the characteristic corona of large, distinctive spikes in the viral envelopes [2,3]. Such 20 nm complex surface projections also surround the periphery of the SARS-CoV particles [4].

The full-length SARS-CoV S glycoprotein and various soluble fragments have been recently cloned, expressed, and characterized biochemically and biophysically [5–10]. S and its soluble ectodomain, S_e, were not cleaved to any significant degree [5]. Cells expressing S fused with receptor-expressing cells at neutral pH, suggesting that the recombinant glycoprotein is functional, its membrane fusogenic activity does not

* Corresponding author. Fax: +1 301 846 5598.
E-mail address: dimitrov@ncifcrf.gov (D.S. Dimitrov).

0006-291X/$ - see front matter © 2004 Elsevier Inc. All rights reserved.
doi:10.1016/j.bbrc.2004.07.084

require other viral proteins, and that low pH is not required for triggering membrane fusion [5]. This observation classifies the SARS-CoV S protein as an exception to the rule that class I fusion proteins are cleaved exposing an N-terminal fusogenic sequence (fusion peptide as was recently demonstrated for other coronaviruses [11]) although cleavage of S could enhance fusion [8].

Because S is not cleaved it is difficult to define the exact location of the boundary between S1 and S2; presumably it is between residues around 672 and 758 [5,6]. Computer analysis suggested the existence of two heptad repeats; peptides from the N- and C-terminal regions of S2 (NP and CP, respectively) can form stable complexes (six-helix bundle structures), indicating that as for other class I fusion proteins such structures are an important intermediate in the fusion process [12–15] and could imply the existence of trimerization domains in the prefusion state.

Fragments containing the N-terminal amino acid residues 17–537 and 272–537 but not 17–276 bound specifically to Vero E6 cells and purified soluble receptor molecules. Together with data for inhibition of binding by antibodies developed against peptides from S, these findings suggested that the receptor-binding domain (RBD) is located between amino acid residues 303 and 537 [5]. Two other groups obtained similar results and found that independently folded fragments as short as 193 residues can specifically bind receptor molecules [7,9].

The function of the region upstream of the receptor binding domain remains unknown. The oligomerization state of SARS-CoV S glycoprotein has not been characterized biochemically and biophysically, and its role in virus entry has not been elucidated. Here we report the identification of a dimerization domain upstream from the RBD in the extreme N-terminal fragment of the S glycoprotein that may play a role in fusion by an unknown mechanism; however, the S ectodomain forms trimers that could mediate fusion through six-helix bundle intermediates.

Materials and methods

Antibodies and plasmids. The rabbit anti-S serum used in Western blot and FACS analyses, P540, was described previously [5]. The anti-Myc epitope antibody was purchased from Invitrogen (Carlsbad, CA). The anti-ACE2 goat polyclonal antibody was purchased from R&D system (Minneapolis, MN) and used for detection by Western blotting. Site directed mutagenesis was used to create the consensus cleavage sites corresponding to that of the HIV-1 envelope glycoprotein (Env) and some coronaviruses within the full length SARS-CoV S glycoprotein gene in pCDNA3. The QuickChange Kit from Stratagene (La Jolla, CA) was used and the protocol suggested by manufacturer was followed. For expression of various N-terminal S fragments, the corresponding gene fragments were amplified by PCR and cloned into the pSecTag2 expression vector (Invitrogen, Carlsbad). The plasmid pCDNA3-ACE2-ecto, which expresses the ACE2 soluble ecto domain tagged with C9 peptide, was kindly provided by Michael Farzan (Harvard University, Boston, MA).

Protein expression and purification. Various N-terminal fragments of the S glycoprotein were sub-cloned in pSecTag2 expression vector and transfected into 293T cells followed by infection with VTF7.3 as described previously [5]. The protein expressed and secreted into the medium was purified using the HiTrap Ni^{2+}-Chelating column (Pharmacia) under the native condition. The purified protein was dialyzed against PBS buffer and stored for further analysis.

S glycoprotein dimerization and its interaction with ACE2 examined by co-immunoprecipitation. For S fragment dimerization, different S glycoprotein constructs were transfected alone or in combination with 293T cells as described previously [5]. Medium containing S fragments was subjected to immunoprecipitation with rabbit anti-S polyclonal antiserum P540. For some co-immunoprecipitation experiments, DTT was added to create reducing condition to eliminate inter-molecule interactions through disulfide bonds. Immunoprecipitated S fragments were detected by Western using an anti-Myc epitope monoclonal antibody. Soluble ACE2-C9 was expressed similarly to expression of S fragments. ACE2-C9 secreted into the medium was used directly for incubation with various S fragments for 2 h at 4 °C. Afterwards, ACE2 was immunoprecipitated by incubating with 1D4 anti-C9 monoclonal antibody and protein G–Sepharose beads at 4 °C for 1 h. The beads were washed four times with PBS, suspended in SDS–PAGE sample buffer, boiled for 3 min, and subjected to gel separation. The presence of either ACE2 or S in the sample was examined by Western as described previously [5].

Flow cytometry. Cells transfected with full length S glycoprotein or S glycoprotein with different N-terminal deletions and infected with VTF7.3 were incubated with the P540 rabbit anti-S polyclonal antibody and goat anti-rabbit antibody conjugated with FITC in PBS containing 1% BSA at 4 °C for 2 h. Cells were then washed four times in ice-cold PBS and analyzed with FacsCalibur (Becton–Dickinson, San Jose, California).

Gel filtration analysis of S fragments. After being purified on Ni-Chelating column and buffer-exchanged to PBS, S fragment samples were loaded onto a Superose 12 10/300 GL column (Pharmacia, Uppsala, Sweden) that had been pre-equilibrated with PBS. The proteins were eluted with PBS at 0.5 ml/min and 0.5 ml fractions were collected. The Superose 12 column was calibrated with protein molecular mass standard of 669, 440, 232, 158, 67, 44, and 25 kDa. A 10 μl aliquot was taken from each fraction for Western blot analysis.

Crosslinking. Purified S537 fragment was diluted to a concentration of 0.2 μg/ml in PBS. BS^3 (Pierce, Rockford, IL) was added to the S537 solution to a final concentration of 1 mg/ml and incubated on ice for 1 min. The samples were then mixed with an equal volume of 4× SDS–PAGE loading buffer and analyzed by Western blot.

Cell fusion β-gal reporter gene assay. Cells transfected with pSecTag2B-S or pCDNA3-ACE2 and infected with VTF7.3 and VCB21R, respectively, were collected by trypsin digestion and washed once with PBS. Cells were then suspended in regular DMEM at pH 7.4 and mixed. Cells were lysed after 4 h of incubation and β-gal activity was measured using CPRG as the substrate (Roche) as previously described [5].

ELISA. Two ELISAs were used. In the sandwich ELISA the plate was coated with an anti-His tag antibody, then the S fragments were added and detected with an anti-c-Myc epitope antibody. This assay was used for detection of the S fragments. In the second ELISA the C9 tagged receptor ACE2 was coated on the plates through an anti-C9 antibody (ID4) and the S fragments were added and after washing detected with an anti-c-Myc epitope antibody. In all experiments the incubations with the c-Myc epitope antibody were for 2 h at room temperature. The optical density (OD) was measured and normalized to the highest value.

Results

The N-terminal fragment upstream of the RBD of the S glycoprotein forms a dimer

It has been previously shown for another coronavirus (MHV) that soluble S1 (equivalent to SU) fragments form dimers, that the extreme N-terminal 330 amino acid residue region that contains the RBD participates in the dimerization, and that only dimers bind the receptor CEACAM [16]. However, we and others have previously localized the SARS-CoV RBD downstream from the extreme N-terminus [5,7,9]. To address the possibility for oligomerization of RBD-containing fragments and their function in mediating membrane fusion we used our previously described fragments [5] including the one from the extreme N-terminus (residues 17 through 276 denoted as S276) which does not bind the receptor ACE2 and several (S756, S537, and S272–537) which bind it as well as another one from residue 317 through 517 denoted as S317–517 that still retains receptor binding activity. These fragments were also selected because they fold independently and are secreted in the cell culture supernatant although the efficiency of their expression varied significantly (Fig. 1A, left) and their concentration was decreased when coexpressed with S756 (Fig. 1A, right).

To find whether any of these fragments oligomerizes with the largest one (S756) that includes the equivalent of the receptor-binding subunit of the envelope glycoproteins (SU in general and S1 for coronaviruses) we coexpressed them, and then immunoprecipitated the mixtures in the cell culture supernatants with the antibody P540. This rabbit polyclonal antibody was developed against a peptide containing residues 540–555 of the S glycoprotein [5] and binds S756 but not the other fragments (Fig. 1B, left). All N-terminal fragments except the smallest fragment (S317–517) containing the RBD were co-immunoprecipitated with S756 by P540 (Fig 1B, right). To rule out the possibility for nonspecific disulfide bond formation that may lead to co-immunoprecipitation, DTT was included in one of the co-immunoprecipitation experiments with no effect on both immunoprecipitation and co-immunoprecipitation of secreted S756 (left lanes) or S756 + S276 (right lanes) (Fig. 1C, left panel).

To find the size of the oligomers we cross-linked one of the fragments (S537) with BS^3. The right panel of Fig. 1C shows the appearance of a new band with a molecular weight corresponding to a dimer but not of higher order oligomers. To exclude the possibilities for artifacts due to cross-linking and further confirm the formation of dimers, the S537 fragment was also analyzed by gel filtration. Two elution peaks were observed: one due to species of molecular weight of about 230 kDa and the other one—of about 110 kDa (Fig. 2A, upper panel) corresponding presumably to a dimer and a monomer.

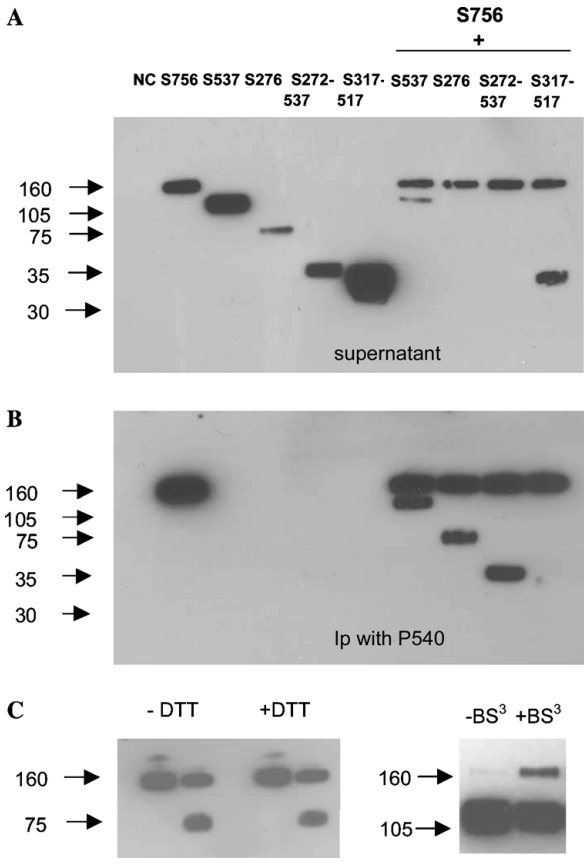

Fig. 1. Dimerization of the N-terminal fragments of the SARS-CoV S glycoprotein demonstrated by co-immunoprecipitation and cross-linking. (A) Plasmids encoding N-terminal fragments (denoted by the number of the ending amino acid residue or the number of the starting and ending residues) were used to transfect alone (left six lanes) or in combination (right four lanes) 293T cells, which were then infected with the vaccinia virus VTF7.3. The culture medium was collected and subjected to Western blot analysis using a mouse anti-c-Myc epitope antibody that recognizes all fragments. (B) The same medium samples used in (A) were subjected first to immunoprecipitation with a polyclonal antibody (P540) that recognizes only S756. The immunoprecipitates were then subjected to Western blot analysis using the same anti-c-Myc epitope antibody. (C) Left panel: medium samples containing secreted S756 (left lanes) or S756 + S276 (right lanes) fragments were subjected to immunoprecipitation with P540 in the presence or absence of 2 mM DTT. Right panel: purified S537 fragment was cross-linked as described in the Materials and methods. In both cases Western was performed with the anti-c-Myc epitope antibody.

In contrast, the smallest fragment containing the RBD (S317–517) was eluted only as a monomer at about 35 kDa molecular weight (Fig. 2A, lower panel). Overall, these results suggest that soluble SU is a dimer and that the dimerization domain is within the extreme N-terminal region upstream from residue 317 and the RBD.

The dimeric N-terminal region is required for S-mediated cell–cell fusion

Because the putative dimerization domain is upstream from the RBD and the fusion machinery is in

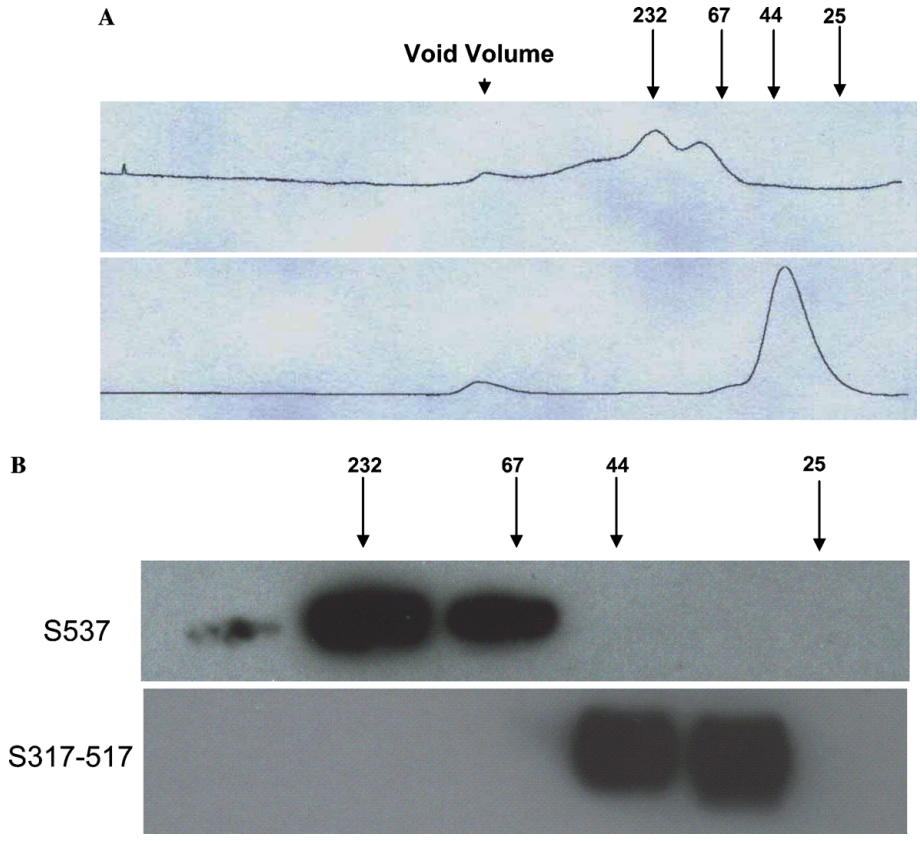

Fig. 2. Dimerization of the N-terminal fragment S537 demonstrated by size-exclusion chromatography. (A) Elution profiles of S537 and S317–517. Arrows and numbers indicate the position at which standard calibration proteins were eluted and their molecular weights. (B) Western blots of fractions collected for S537 and S317–517 by using an anti-c-Myc epitope antibody.

S2, one might hypothesize that it may not be required for mediation of fusion. To test this hypothesis we generated two deletion mutants of the full-length S glycoprotein where 103 and 311 N-terminal residues were deleted (Fig. 1A) presumably eliminating the dimerization domain. Both mutants did not exhibit any fusion activity compared to the wild type full-length S glycoprotein which did (Fig. 1A). To test whether differential level of expression could account for lack of observable fusogenic activity we measured the surface and overall levels of expression by flow cytometry and Western blotting. The data from both assays suggested that the level of expression of the two deletion mutants is undistinguishable from that of the wild type (Figs. 3B and C). These results suggest that the extreme N-terminus is required for fusion by a mechanism that may or may not involve dimerization.

Dimeric S1 binds ACE2 much more efficiently than monomeric fragments containing the RBD

In light of previous work with another coronavirus (MHV) [16] suggesting that only dimeric S1 binds its receptor CEACAM and to begin to understand how the dimeric state of the S1 may affect fusion, we measured binding of S1 fragments in monovalent and bivalent forms by using the anti-c-Myc epitope antibody for conversion of monovalent fragments into bivalent ones. One of these fragments (S319–517) did not bind to any measurable degree to surface immobilized ACE2 unless bound by an anti-c-Myc epitope antibody (converting it into a bivalent molecule) in solution before and during incubation with the receptor (Fig. 4). In contrast, S537 bound to ACE2 without the antibody although the antibody presence increased its binding (Fig. 4). These results suggest that a dimeric state of S1 could contribute to an increased overall affinity that may enhance fusion efficiency.

The soluble S ectodomain is a trimer

Viral envelope glycoproteins of class I fusion proteins such as HA of influenza are trimeric through the TM subunit. Because the SARS-CoV S glycoprotein was recently found to be class I fusion protein it appears likely that the S2 subunit would confer a trimeric state to the whole S glycoprotein. However, a dimeric state of S1 with a trimeric S2 could theoretically lead to higher order oligomers in dependence on the availability of the dimerization binding site in the context of the native S glycoprotein. To test such a possibility we measured

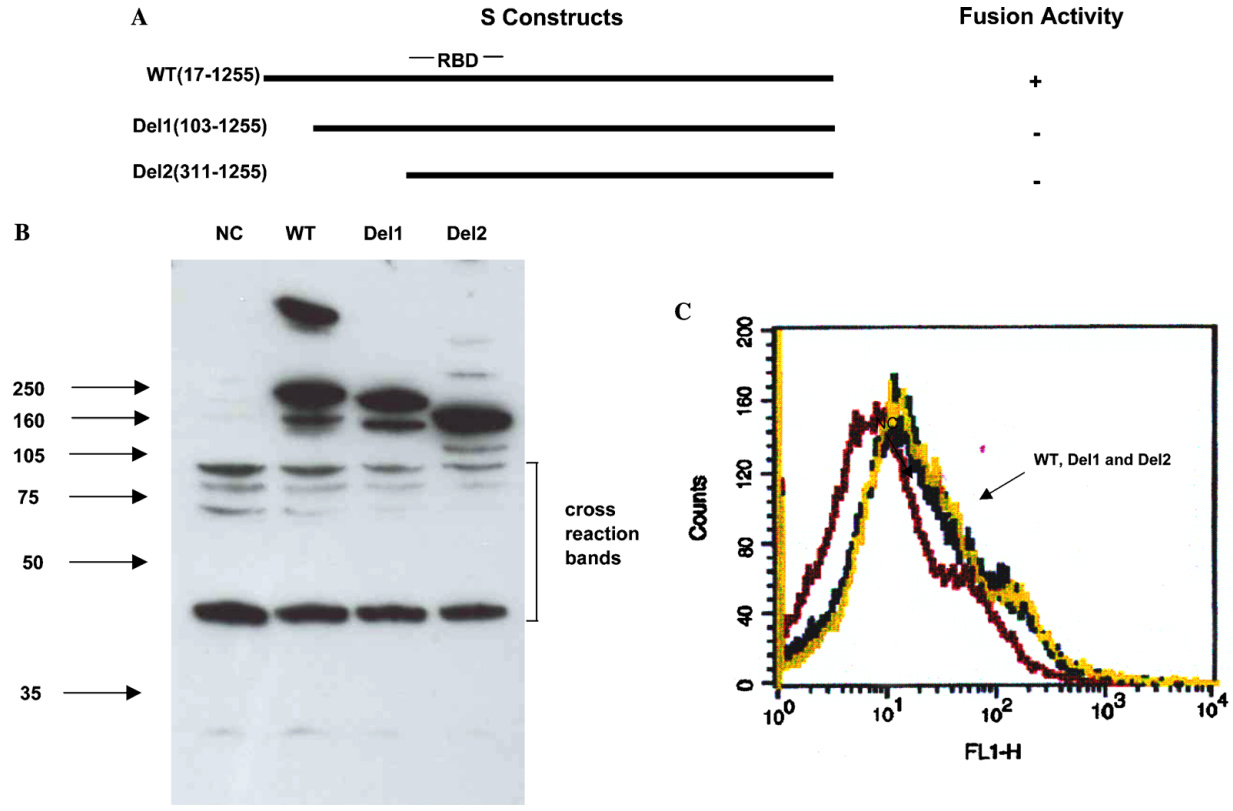

Fig. 3. The extreme N-terminus is required for the S glycoprotein-mediated cell–cell fusion. (A) Schematic representation of the S glycoprotein deletion mutants and a summary of the data from a cell–cell fusion assay where RBD denotes the approximate position of the receptor binding domain. Presence of signal due to fusion is denoted by + and lack of measurable signal above the background value by −. (B) Levels of expression of full length and deletion mutants of the S glycoprotein measured by Western. Equal amounts of cell lysates were loaded for each sample and the rabbit polyclonal antibody P540 was used for detection. (C) Cell surface expression of the full length and deletion mutants of the S glycoprotein measured by flow cytometry. The level of surface expression is low although the negative control where the cells were transfected with an empty plasmid is clearly distinguishable on left of the other three curves.

approximately the size of the soluble S ectodomains (Se) where the transmembrane domain and the cytoplasmic tail were deleted [5] by gel filtration. The data shown in Fig. 5 demonstrate the existence of a trimeric state of Se (Mw 512 kDa) and lack of higher order oligomers. These results not only suggest that the Se and perhaps the full-length membrane-associated S are trimers in their native unbound state but also indicate that the dimerization site in S1 is not readily available for inter-trimer interactions.

Discussion

Major findings of this work are that (i) the SU subunit of the SARS-CoV S glycoprotein (S1) forms dimers, (ii) the dimerization domain does not overlap and is upstream of the RBD, (iii) its deletion abolishes fusion, (iv) dimeric S1 binds receptor molecules much more efficiently than monovalent fragments containing the RBD, and (v) the soluble S ectodomain forms trimers under gel filtration conditions.

It has been previously reported that some attachment SU subunits of class I fusion proteins that bind receptor molecules can form dimers including gp120 of the retrovirus HIV-1 [17] and S1 of the coronavirus MHV [16]. What is the role of S1 dimerization for mediation of membrane fusion however remains unclear. It is now generally accepted that soluble ectodomains (gp140) of the HIV-1 and SIV envelope glycoproteins (Env) form trimers [18] although dimers and tetramers can be observed [19]. Similarly, it appears that at least a possible fusion intermediate quaternary structure of coronaviruses including the SARS-CoV of S2 is trimeric [12,13]. However, remarkably it was reported that the MHV S2 protein is monomeric after dissociation from S1 [16]. Dimer-to-trimer transitions play a critical role in the mechanism of fusion mediated by class II fusion proteins. Thus, it has been proposed that changes in the quaternary structure of some coronaviruses may play a role in the fusion mechanism [16]. One should note that both the HIV-1 Env and the MHV S glycoprotein are cleaved and the SU can dissociate from the TM subunit although such dissociation may not be important for

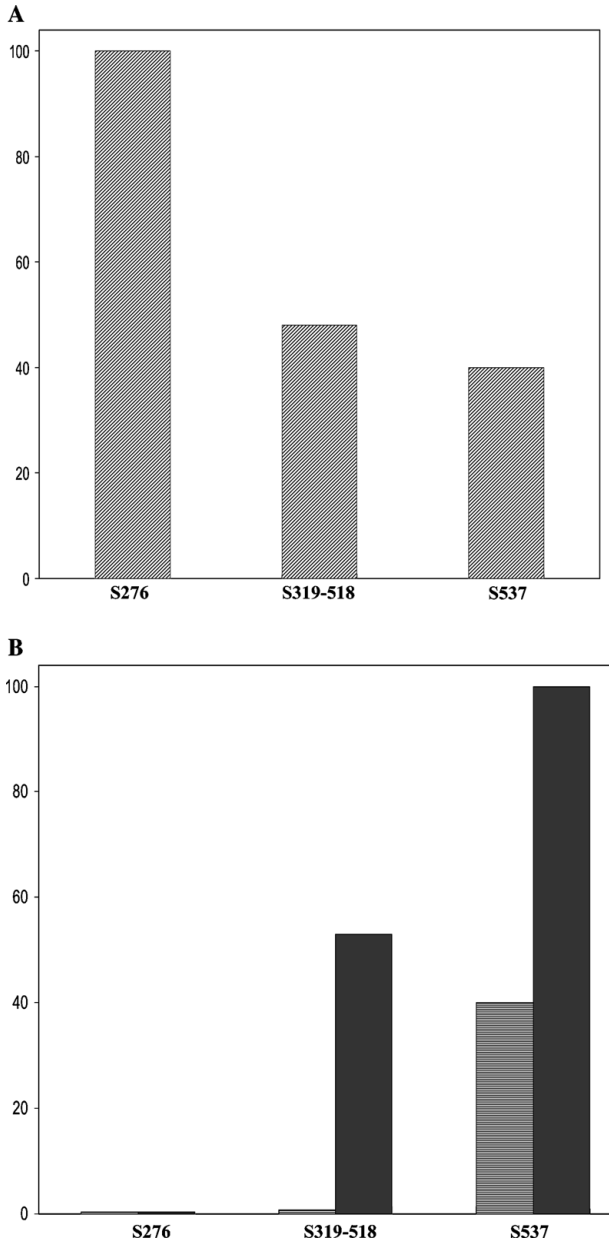

Fig. 4. Dimeric S1 binds much more efficiently the receptor ACE2 than monovalent fragments containing the RBD. (A) Measurement of the level of expression of different S fragments by ELISA in 200 μl of culture supernatants of cells transfected with various constructs. Anti-His and anti-c-Myc epitope antibodies were used in a sandwich ELISA to detect the levels of secreted tagged S proteins. (B) Binding of S fragments to ACE2 measured by ELISA. The tagged ACE2 was associated to the plate by an anti-C9 antibody coated on the plates. The supernatants from cell cultures where the cells were transfected with various S proteins and that with ACE 2 were mixed and incubated in ELISA plates either with (solid black bars) or without (hatched bars) anti-c-Myc antibody. The highest level of expression or binding is assumed to be 100%.

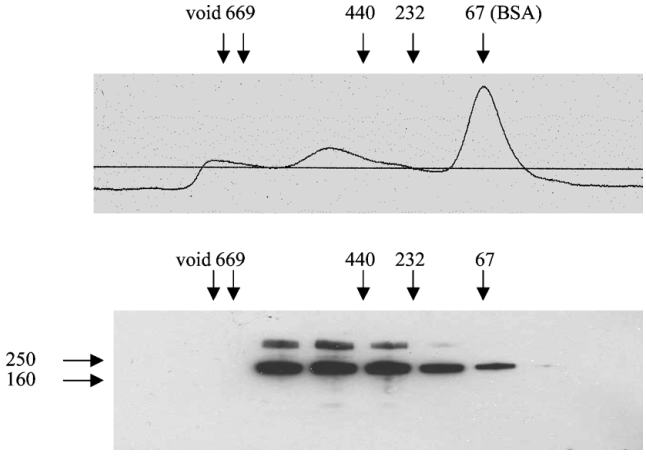

Fig. 5. The soluble S ectodomain is trimeric under the conditions of size-exclusion chromatography. (A) Purified Se was run on a gel filtration column that was calibrated by using proteins with known molecular weight. BSA in equal amount was included as an internal control. (B) Different fractions were collected and analyzed by Western blot. Note that the two bands in each lane represent the Se (lower band) and its aggregates (upper band) as also seen in Fig. 3 with the full length native S glycoprotein.

fusion. In contrast, the SARS-CoV S is not cleaved when expressed in membrane associated or soluble form and cleavage may not be required for fusion. Thus, although the SARS-CoV S glycoprotein is a class I fusion protein, the lack of cleavage is an exception from the rule that the Envs of class I fusion proteins are cleaved presumably to confer a metastable high-energy state that could drive the fusion reaction.

Our finding that the SU of the SARS-CoV S glycoprotein can form dimers but the soluble ectodomain of the Env that includes SU and the ectodomain of the TM (S2) forms trimers poses an interesting topological situation. Even if in the trimer two of the monomers form a dimer, then the third one could be free to interact with a "free" monomer from another trimer and form a dimer of trimers. In another possible scenario the orientation of each of the monomers in the trimer may not allow formation of dimers in the trimer but leave "free" binding sites for dimerization with monomers from other trimers. In this case one might expect the formation of a network of trimers. Finally, the three-dimensional structure of the trimer may not allow any interactions of the monomer dimerization sites with other monomers in the same or different trimer. We have not observed higher order oligomers under our gel filtration conditions indicating that under those conditions either intratrimer dimerization occurs but the third monomer conformation does not allow interactions with monomers from other trimers or such interactions are too weak to be detected, or the trimer three-dimensional structure is such that it does not allow dimerization interactions.

However, our data demonstrating lack of fusion after deletion of portions of the dimerization domain indicate that the dimerization region may play a role in fusion although its mechanism may not be through dimerization

interactions. In addition, under native conditions where the surface concentration of the S glycoprotein can be very high, as seen in electron micrographs, it is possible that dimerization interactions play a role in stabilizing a "network" of interacting molecules perhaps somewhat similar to networks of proteins that mediate entry of class II fusion proteins. Such networks, if any, could increase the avidity of interaction with receptor molecules and perhaps facilitate the formation of the fusion pore structure by providing a preassembled network of Env molecules or even provide energy to drive the fusion reaction in the absence of S cleavage that generates a high-energy metastable state. Further experiments are needed to test the validity of such a hypothesis, which in the absence of data directly supporting it remains highly speculative.

Note added in proof

In a recent article (J. Virol. 78 (2004) 7217–7226) Zhou also reported a trimeric form of the S protein.

Acknowledgments

We thank the members of our group Protein Interactions for helpful discussions and M. Farzan for providing the plasmid encoding ACE2.

References

[1] D.S. Dimitrov, Virus entry: molecular mechanisms and biomedical applications, Nat. Rev. Microbiol. 2 (2004) 109–122.
[2] K.V. Holmes, SARS-associated coronavirus, N. Engl. J. Med. 348 (2003) 1948–1951.
[3] M.M. Lai, D. Cavanagh, The molecular biology of coronaviruses, Adv. Virus Res. 48 (1997) 1–100.
[4] T.G. Ksiazek, D. Erdman, C.S. Goldsmith, S.R. Zaki, T. Peret, S. Emery, S. Tong, C. Urbani, J.A. Comer, W. Lim, P.E. Rollin, S.F. Dowell, A.E. Ling, C.D. Humphrey, W.J. Shieh, J. Guarner, C.D. Paddock, P. Rota, B. Fields, J. DeRisi, J.Y. Yang, N. Cox, J.M. Hughes, J.W. LeDuc, W.J. Bellini, L.J. Anderson, A novel coronavirus associated with severe acute respiratory syndrome, N. Engl. J. Med. 348 (2003) 1953–1966.
[5] X. Xiao, S. Chakraborti, A.S. Dimitrov, K. Gramatikoff, D.S. Dimitrov, The SARS-CoV S glycoprotein: expression and functional characterization, Biochem. Biophys. Res. Commun. 312 (2003) 1159–1164.
[6] W. Li, M.J. Moore, N. Vasilieva, J. Sui, S.K. Wong, M.A. Berne, M. Somasundaran, J.L. Sullivan, K. Luzuriaga, T.C. Greenough, H. Choe, M. Farzan, Angiotensin-converting enzyme 2 is a functional receptor for the SARS coronavirus, Nature 426 (2003) 450–454.
[7] S.K. Wong, W. Li, M.J. Moore, H. Choe, M. Farzan, A 193-amino acid fragment of the SARS coronavirus S protein efficiently binds angiotensin-converting enzyme 2, J. Biol. Chem. 279 (2004) 3197–3201.
[8] G. Simmons, J.D. Reeves, A.J. Rennekamp, S.M. Amberg, A.J. Piefer, P. Bates, Characterization of severe acute respiratory syndrome-associated coronavirus (SARS-CoV) spike glycoprotein-mediated viral entry, Proc. Natl. Acad. Sci. USA 101 (2004) 4240–4245.
[9] G.J. Babcock, D.J. Esshaki, W.D. Thomas Jr., D.M. Ambrosino, Amino acids 270 to 510 of the severe acute respiratory syndrome coronavirus spike protein are required for interaction with receptor, J. Virol. 78 (2004) 4552–4560.
[10] H. Bisht, A. Roberts, L. Vogel, A. Bukreyev, P.L. Collins, B.R. Murphy, K. Subbarao, B. Moss, Severe acute respiratory syndrome coronavirus spike protein expressed by attenuated vaccinia virus protectively immunizes mice, Proc. Natl. Acad. Sci. USA 101 (2004) 6641–6646.
[11] B.J. Bosch, Z.R. van der, C.A. de Haan, P.J. Rottier, The coronavirus spike protein is a class I virus fusion protein: structural and functional characterization of the fusion core complex, J. Virol. 77 (2003) 8801–8811.
[12] S. Liu, G. Xiao, Y. Chen, Y. He, J. Niu, C.R. Escalante, H. Xiong, J. Farmar, A.K. Debnath, P. Tien, S. Jiang, Interaction between heptad repeat 1 and 2 regions in spike protein of SARS-associated coronavirus: implications for virus fusogenic mechanism and identification of fusion inhibitors, Lancet 363 (2004) 938–947.
[13] B.J. Bosch, B.E. Martina, Z.R. van der, J. Lepault, B.J. Haijema, C. Versluis, A.J. Heck, R. de Groot, A.D. Osterhaus, P.J. Rottier, Severe acute respiratory syndrome coronavirus (SARS-CoV) infection inhibition using spike protein heptad repeat-derived peptides, Proc. Natl. Acad. Sci. USA 101 (2004) 8455–8460.
[14] J. Zhu, G. Xiao, Y. Xu, F. Yuan, C. Zheng, Y. Liu, H. Yan, D.K. Cole, J.I. Bell, Z. Rao, P. Tien, G.F. Gao, Following the rule: formation of the 6-helix bundle of the fusion core from severe acute respiratory syndrome coronavirus spike protein and identification of potent peptide inhibitors, Biochem. Biophys. Res. Commun. 319 (2004) 283–288.
[15] B. Tripet, M.W. Howard, M. Jobling, R.K. Holmes, K.V. Holmes, R.S. Hodges, Structural characterization of the SARS-coronavirus spike S fusion protein core, J. Biol. Chem. 279 (2004) 20836–20849.
[16] D.N. Lewicki, T.M. Gallagher, Quaternary structure of coronavirus spikes in complex with carcinoembryonic antigen-related cell adhesion molecule cellular receptors, J. Biol. Chem. 277 (2002) 19727–19734.
[17] R.J. Center, P.L. Earl, J. Lebowitz, P. Schuck, B. Moss, The human immunodeficiency virus type 1 gp120 V2 domain mediates gp41-independent intersubunit contacts, J. Virol. 74 (2000) 4448–4455.
[18] R.J. Center, P. Schuck, R.D. Leapman, L.O. Arthur, P.L. Earl, B. Moss, J. Lebowitz, Oligomeric structure of virion-associated and soluble forms of the simian immunodeficiency virus envelope protein in the prefusion activated conformation, Proc. Natl. Acad. Sci. USA 98 (2001) 14877–14882.
[19] P.L. Earl, B. Moss, Mutational analysis of the assembly domain of the HIV-1 envelope glycoprotein, AIDS Res. Hum. Retroviruses 9 (1993) 589–594.